

# Mitigating Hallucinations in Video Large Language Models via Spatiotemporal-Semantic Contrastive Decoding

Yuansheng Gao<sup>1</sup> Jinman Zhao<sup>2</sup> Tong Zhang<sup>1</sup> Xingguo Xu<sup>3</sup> Han Bao<sup>1</sup> Zonghui Wang<sup>1</sup> Wenzhi Chen<sup>1</sup>

## Abstract

Although Video Large Language Models perform remarkably well across tasks such as video understanding, question answering, and reasoning, they still suffer from the problem of hallucination, which refers to generating outputs that are inconsistent with explicit video content or factual evidence. However, existing decoding methods for mitigating video hallucinations, while considering the spatiotemporal characteristics of videos, mostly rely on heuristic designs. As a result, they fail to precisely capture the root causes of hallucinations and their fine-grained temporal and semantic correlations, leading to limited robustness and generalization in complex scenarios. To more effectively mitigate video hallucinations, we propose a novel decoding strategy termed Spatiotemporal-Semantic Contrastive Decoding. This strategy constructs negative features by deliberately disrupting the spatiotemporal consistency and semantic associations of video features, and suppresses video hallucinations through contrastive decoding against the original video features during inference. Extensive experiments demonstrate that our method not only effectively mitigates the occurrence of hallucinations, but also preserves the general video understanding and reasoning capabilities of the model.

## 1. Introduction

The advancement of Video Large Language Models (VideoLLMs) has greatly accelerated progress in open-ended tasks such as video understanding, question answering, and reasoning (Li et al., 2025a; Xu et al., 2024; Ma et al., 2024; Cui et al., 2025; Wang et al., 2025). However, hallucination has emerged as a key issue that undermines their reliability and trustworthiness (Sun et al., 2025; Poppi et al., 2026; Gao

et al., 2025a; Tang et al., 2025). Specifically, hallucinations manifest as cases where the model generates semantically coherent descriptions that are inconsistent with the input video content or factual evidence (Liu et al., 2024b; Zheng et al., 2024). Although numerous studies have focused on mitigating hallucinations in images (Fang et al., 2025; Yue et al., 2024; Jiang et al., 2025; Gunjal et al., 2024; Fu et al., 2025; Liu et al., 2024a), relatively few efforts have been devoted to mitigating video hallucinations.

Current research on mitigating hallucinations in VideoLLMs primarily focuses on the following three aspects: First, several methods rely on preference-based finetuning to discourage hallucinated responses (Ding et al., 2025; Huang et al., 2025), but such approaches depend heavily on large curated preference datasets and significant computational cost. Second, architecture-level modifications (Ma et al., 2024) can improve alignment but typically require re-training or introduce incompatibilities with efficient attention implementations such as FlashAttention (Shah et al., 2024), limiting their scalability. Third, decoding-time or feature-level adjustments (Kong et al., 2025; Zhang et al., 2024a; Li et al., 2025a) help reduce hallucination but often rely on heuristic temporal or saliency cues, which restricts their robustness and generalization across diverse video contexts.

Prior studies have shown that, within the contrastive decoding framework, negative projections that are more prone to inducing hallucinations are more effective at mitigating hallucinations than positive projections (Chen et al., 2025). Inspired by this observation, we focus on the spatiotemporal characteristics specific to videos and their semantic associations with the target text, and propose a novel decoding strategy termed Spatiotemporal-Semantic Contrastive Decoding (SSCD). This method constructs negative video features by deliberately disrupting the spatiotemporal consistency of encoded video features, as well as the semantic alignment between the projected visual tokens and the target text. During inference, these negative features are incorporated into the decoding process to calibrate the model’s sampling distribution, thereby suppressing hallucinations.

To obtain negative video features, we design a lightweight learnable network, termed the Spatiotemporal-Semantic Disruptor. As shown in Figure 1, it operates by applying

<sup>1</sup>Zhejiang University <sup>2</sup>University of Toronto <sup>3</sup>Dalian University of Technology. Correspondence to: Yuansheng Gao <y.gao@zju.edu.cn>.

residual perturbations to video features, thereby disrupting both their spatiotemporal and semantic representations. To disrupt spatiotemporal consistency, we model the encoded video features of each video frame as nodes in a graph and establish connections between adjacent frames, thereby constructing a spatiotemporal graph structure. Inspired by [Jabri et al. \(2020\)](#), we perform random walks on the spatiotemporal graph to disrupt the spatiotemporal consistency of video features by weakening cross-temporal and cross-spatial associations. To disrupt semantic consistency, we weaken the association between video features and linguistic semantics by minimizing the conditional mutual information ([Zhao et al., 2019](#)) between the video tokens obtained by projecting video features and the target text. SSCD leverages video features with deliberately disrupted spatiotemporal and semantic consistency to construct a contrastive decoding process, thereby effectively mitigating video hallucinations. In summary, our main contributions are:

- We construct negative video features that are prone to inducing hallucinations in VideoLLMs from two perspectives: disrupting the spatiotemporal consistency of video representations and weakening their semantic alignment with target text.
- To mitigate hallucinations, we introduce the constructed negative video features as contrastive signals into the decoding process, where they serve as a counterpoint to the original video features, leading to a strategy termed SSCD.
- Extensive experiments demonstrate that the proposed method not only effectively mitigates video hallucinations, but also preserves the general video understanding and reasoning capabilities of VideoLLMs.

## 2. Related Work

### 2.1. Video Large Language Models

In recent years, VideoLLMs have achieved remarkable progress in the field of multimodal understanding across vision and language ([Bagad et al., 2023](#); [Zhang et al., 2025](#)). Early studies were largely extensions of image-language models such as CLIP ([Radford et al., 2021](#)) and BLIP ([Li et al., 2022](#)), aligning video frames with textual descriptions or questions through frame-level feature aggregation or cross-modal attention mechanisms. With the emergence of Large Language Models (LLMs) ([Zhao et al., 2025a](#); [Yuan et al., 2025a](#); [Gao et al., 2025b](#); [Yuan et al., 2025b](#)), recent works further couple powerful LLM backbones with video encoders, yielding instruction-following VideoLLMs capable of open-ended reasoning and dialogue ([Gao et al., 2023](#); [Zhang et al., 2023](#)). These models, such as VideoLLaVA ([Lin et al., 2024](#)), VideoChatGPT ([Maaz et al.,](#)

[2024](#)), and Valley ([Wu et al., 2025b](#)), typically process spatiotemporal visual tokens extracted from pretrained video encoders (e.g., CLIP, LanguageBind ([Zhu et al., 2024](#))) and inject them into LLMs through lightweight projection layers for multimodal alignment. Despite their strong performance, current VideoLLMs remain prone to video hallucination ([Zhang et al., 2024a](#)). Our work aims to mitigate this issue and enhance the reliability of VideoLLMs.

### 2.2. Hallucination in Video Large Language Models

Hallucination in VideoLLMs typically refers to the phenomenon where the generated outputs are inconsistent with salient visual information or objective factual evidence present in the video ([Li et al., 2025a](#); [Bae et al., 2025](#)). Prior studies on image hallucination mainly fall into two categories: post-processing approaches ([Leng et al., 2024](#); [Li et al., 2025b](#); [Lee et al., 2024](#); [Yuan et al., 2024](#); [Chen et al., 2025](#)) and data-driven preference alignment ([Yu et al., 2024](#); [Liu et al., 2024a](#)). The former refines model outputs after generation, whereas the latter leverages the Direct Preference Optimization (DPO) ([Rafailov et al., 2023](#)) framework to reduce hallucination by improving dataset quality or optimizing preference learning. Compared with static images, the temporal dynamics of videos pose greater challenges for hallucination mitigation ([Wang et al., 2024](#)). PaMi-VDPO ([Ding et al., 2025](#)) and VistaDPO ([Huang et al., 2025](#)) apply DPO-based post-training to promote faithful responses, yet their reliance on large curated preference datasets entails substantial computational and annotation costs. VISTA-LLAMA ([Ma et al., 2024](#)) modifies the attention mechanism by removing relative positional encoding between visual and textual tokens to maintain a consistent influence of visual tokens during generation, but does not explicitly model causal reasoning. Methods such as MotionCD ([Kong et al., 2025](#)), Dino-Heal ([Zhang et al., 2024a](#)), and TCD ([Li et al., 2025a](#)) mitigate hallucinations by introducing inference-time interventions, including motion-aware contrastive signals and video feature reweighting. Although these approaches demonstrate performance gains, their designs are primarily heuristic and lack a unified theoretical characterization, which limits their robustness and generalization across tasks and settings.

## 3. Preliminary

Before introducing SSCD, we briefly review the general formulation of VideoLLMs and the autoregressive generation mechanism commonly adopted during inference.

### 3.1. Video-Language Model Formulation

A typical VideoLLM consists of a video encoder, a multimodal projector, and a LLM. Given an input video  $V = \{v_1, v_2, \dots, v_T\}$  consisting of  $T$  frames, the video encoder

$\mathcal{E}_v(\cdot)$  extracts spatiotemporal video features:

$$\mathbf{H}_v = \mathcal{E}_v(V) \in \mathbb{R}^{T \times N \times d}, \quad (1)$$

where  $N$  denotes the number of visual tokens per frame and  $d$  is the feature dimension. These video features are then mapped into the language embedding space through a projection module  $\mathcal{P}(\cdot)$ :

$$\mathbf{Z}_v = \mathcal{P}(\mathbf{H}_v). \quad (2)$$

The projected video tokens  $\mathbf{Z}_v$  are concatenated with textual tokens (e.g., questions or instructions) and fed into the LLM, which performs multimodal reasoning and generates textual outputs in an autoregressive manner.

### 3.2. Autoregressive Decoding in VideoLLMs

Given the projected visual tokens  $\mathbf{Z}_v$  and a textual prompt  $\mathbf{X} = \{x_1, \dots, x_m\}$ , the LLM defines a conditional probability distribution over a response sequence  $\mathbf{Y} = \{y_1, \dots, y_L\}$  in an autoregressive manner:

$$p_\theta(\mathbf{Y} \mid \mathbf{Z}_v, \mathbf{X}) = \prod_{t=1}^L p_\theta(y_t \mid \mathbf{Z}_v, \mathbf{X}, y_{<t}). \quad (3)$$

where,  $p_\theta(\cdot)$  denotes the conditional distribution over text tokens induced by the LLM parameterized by  $\theta$  given multimodal inputs.

At decoding step  $t$ , the conditional probability of generating the next token  $y_t$  is given by:

$$p_\theta(y_t \mid \mathbf{Z}_v, \mathbf{X}, y_{<t}) = \text{Softmax}(f_\theta(\mathbf{Z}_v, \mathbf{X}, y_{<t})), \quad (4)$$

where  $f_\theta$  denotes the output logits of the LLM parameterized by  $\theta$ . Although autoregressive decoding enables flexible and fluent generation, it is prone to hallucination in multimodal settings: weakly grounded tokens can propagate and amplify through subsequent steps, yielding fluent yet visually inconsistent outputs.

## 4. Methodology

To mitigate hallucination in VideoLLMs, we propose SSCD (see Figure 1), a decoding strategy that constructs negative video features along two dimensions: (i) Spatiotemporal Consistency Disruption: by leveraging random walks to deliberately break spatiotemporal consistency across frames, we construct negative video features with disrupted temporal structures; (ii) Semantic Consistency Disruption: by minimizing the conditional mutual information between the visual tokens obtained from projecting video features and the ground-truth answer, we intentionally weaken their semantic consistency and construct semantically mismatched negative video features.

In practice, we design a lightweight disruptor  $\mathcal{M}$  that perturbs video features in a residual manner. Formally, this process can be expressed as:

$$\mathbf{H}_v^{\text{Neg}} = \mathbf{H}_v + \mathcal{M}(\mathbf{H}_v), \quad (5)$$

where  $\mathbf{H}_v^{\text{Neg}}$  denotes the disrupted video features. After projection, the disrupted video features are transformed into negative visual tokens  $\mathbf{Z}_v^{\text{Neg}} = \mathcal{P}(\mathbf{H}_v^{\text{Neg}})$ . Subsequent sections detail the training procedure of the disruptor  $\mathcal{M}$  and its role during inference.

### 4.1. Spatiotemporal Consistency Disruption

We model the video features as a spatiotemporal graph, where each video feature  $h_k^n \in \mathbf{H}_v^{\text{Neg}}$  corresponds to a node, with  $k$  denoting the frame index and  $n$  denoting the feature index within the frame. Edges connect only features in consecutive frames. Affinity between features in consecutive frames is defined via dot-product similarity:

$$S_k^{k+1}(i, j) = \langle h_k^i, h_{k+1}^j \rangle. \quad (6)$$

A row-wise softmax then yields the transition matrix

$$\mathcal{T}_k^{k+1}(i, j) = \frac{\exp(S_k^{k+1}(i, j)/\tau)}{\sum_{n=1}^N \exp(S_k^{k+1}(i, n)/\tau)}, \quad (7)$$

where  $\tau$  is a temperature parameter that controls the sharpness of the transition distribution.

Inspired by Jabri et al. (2020), we introduce a random-walk mechanism on the spatiotemporal graph to model long-range consistency while deliberately disrupting cross-frame spatiotemporal coherence. Let  $W_k$  denote the state of a random walker at frame  $k$ . Since  $\mathcal{T}_k^{k+1}(i, j) = P(W_{k+1} = j \mid W_k = i)$  specifies the one-step transition probability from node  $u_k^i$  to node  $u_{k+1}^j$ , long-range temporal consistency can be modeled by composing multiple such transitions. By the Markov property, the multi-step transition probability from frame  $k$  to frame  $k+z$  is obtained by marginalizing over all intermediate states, which corresponds exactly to the product of the one-step transition matrices:

$$\bar{\mathcal{T}}_k^{k+z} = \prod_{i=0}^{z-1} \mathcal{T}_{k+i}^{k+i+1} = P(W_{k+z} \mid W_k). \quad (8)$$

Thus,  $\bar{\mathcal{T}}_k^{k+z}$  represents the probability of propagating consistency from frame  $k$  to frame  $k+z$ .

We next characterize cycle consistency across multiple temporal spans for a video with  $T$  frames. For a given span  $z$ , the forward random walk from frame  $k$  to frame  $k+z$  is governed by  $\bar{\mathcal{T}}_k^{k+z}$ , while the corresponding reverse walk along the palindromic sequence is governed by  $(\bar{\mathcal{T}}_k^{k+z})^\top$ . By sequentially composing the forward and reverse walks,

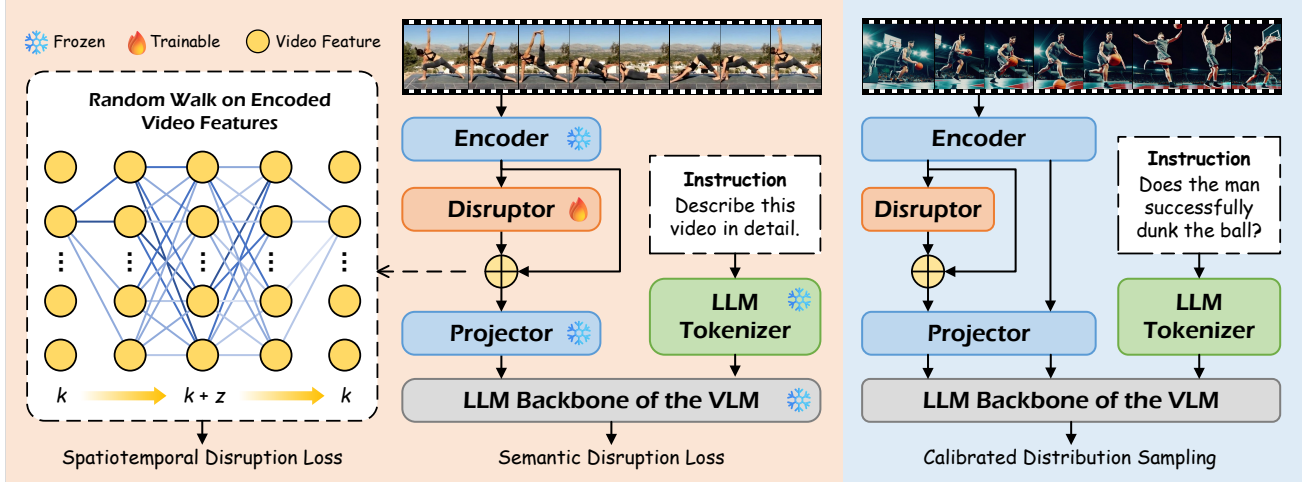


Figure 1. Overview of the proposed SSCD. **Left:** We freeze the VideoLLM and train only a lightweight spatiotemporal-semantic disruptor. **Right:** During inference, we use the trained disruptor to generate negative video features with disrupted spatiotemporal and semantic consistency, and mitigate hallucinations via calibrated distribution sampling with contrastive decoding.

the resulting  $2z$ -step round-trip transition from frame  $k$  back to itself is defined as

$$P(W_{k+2z} | W_k) = \bar{\mathcal{T}}_k^{k+z} (\bar{\mathcal{T}}_k^{k+z})^\top. \quad (9)$$

The diagonal entry of this round-trip transition matrix,  $P(W_{k+2z} = i | W_k = i)$ , corresponds to the probability that a walker starting at feature  $i$  returns to the same token after the  $2z$ -step palindromic walk. Based on the above analysis, to deliberately disrupt cross-frame spatiotemporal consistency, we define a cycle-consistency score as

$$\begin{aligned} c_{k,z} &= \sum_{i=1}^N \log P(W_{k+2z} = i | W_k = i) \\ &= \sum_{i=1}^N \log \left( [\bar{\mathcal{T}}_k^{k+z} (\bar{\mathcal{T}}_k^{k+z})^\top]_{ii} \right), \end{aligned} \quad (10)$$

Subsequently, we compute the cycle-consistency score over all admissible temporal spans  $\mathcal{Z} = \{1, \dots, Z_{\max}\}$ , thereby intentionally introducing and amplifying disruptions of spatiotemporal consistency, where  $Z_{\max} = T - 2$  denotes the largest span for which the palindromic sequence remains entirely within the video. Specifically, for a given span  $z \in \mathcal{Z}$ , the corresponding set of valid starting indices is  $\mathcal{K}_z = \{k | k + 2z \leq T\}$ . The spatiotemporal consistency disruption loss  $\mathcal{L}_T$  is defined as the average cycle-consistency score over all temporal spans and their valid starting indices:

$$\mathcal{L}_T = \frac{1}{\sum_{z \in \mathcal{Z}} |\mathcal{K}_z|} \sum_{z \in \mathcal{Z}} \sum_{k \in \mathcal{K}_z} c_{k,z}. \quad (11)$$

This objective builds on a random-walk formulation over a spatiotemporal graph, explicitly amplifying cycle inconsistency during long-range propagation via the transition

matrix. Furthermore, these inconsistencies across different temporal spans are aggregated, thereby weakening long-term self-consistency in video representations and steering them toward hallucination-prone states during decoding.

## 4.2. Semantic Consistency Disruption

Video features are mapped into the language model’s shared embedding space via a visual projector, enabling visual and textual tokens to be jointly decoded within a unified Transformer (Vaswani et al., 2017). This design provides the foundation for modeling the relationship between video features and language semantics. Moreover, during decoding, when visual representations are semantically misaligned with the correct answer, the language model is more likely to generate content that is inconsistent with the visual evidence (Leng et al., 2024; Chen et al., 2025).

Accordingly, beyond disrupting spatiotemporal coherence, we deliberately disrupt the semantic alignment between video features and the correct answer. Formally, given a dataset  $\mathcal{D}$ , we minimize the conditional mutual information between negative visual tokens  $\mathbf{Z}_v^{\text{Neg}}$  and the answer  $\mathbf{Y}$  conditioned on the input text  $\mathbf{X}$ :

$$\begin{aligned} & \min_{\mathbf{Z}_v^{\text{Neg}}} I(\mathbf{Z}_v^{\text{Neg}}; \mathbf{Y} | \mathbf{X}) \\ &= \min_{\mathbf{H}_v^{\text{Neg}}} I(\mathcal{P}(\mathbf{H}_v^{\text{Neg}}); \mathbf{Y} | \mathbf{X}) \\ &= \min_{\mathbf{H}_v^{\text{Neg}}} (H(\mathbf{Y} | \mathbf{X}) - H(\mathbf{Y} | \mathcal{P}(\mathbf{H}_v^{\text{Neg}}), \mathbf{X})). \end{aligned} \quad (12)$$

Since  $H(\mathbf{Y} | \mathbf{X})$  does not depend on  $\mathbf{H}_v^{\text{Neg}}$ , minimizing the mutual information is equivalent to

$$\min_{\mathbf{H}_v^{\text{Neg}}} -H(\mathbf{Y} | \mathcal{P}(\mathbf{H}_v^{\text{Neg}}), \mathbf{X}). \quad (13)$$



Intuitively, this encourages the projected visual tokens to provide misleading or uninformative signals for predicting the correct answer, thereby breaking semantic consistency between video evidence and answer tokens.

In practice, the conditional entropy is approximated by the log-likelihood under the model distribution:

$$\mathbb{E}_{(\mathbf{X}, \mathbf{Y}, V) \sim \mathcal{D}} \left[ \log p_{\theta}(\mathbf{Y} \mid \mathcal{P}(\mathbf{H}_v^{\text{Neg}}), \mathbf{X}) \right]. \quad (14)$$

Accordingly, for a single example  $(\mathbf{X}, \mathbf{Y}, V)$ , the semantic disruption loss  $\mathcal{L}_S$  can be written as:

$$\mathcal{L}_S = \sum_{t=1}^L \log p_{\theta}(y_t \mid \mathcal{P}(\mathbf{H}_v^{\text{Neg}}), \mathbf{X}, y_{<t}). \quad (15)$$

From a training perspective, this objective reduces the probability of predicting the ground-truth answer under negative video features, thereby weakening the dependence between visual representations and answer semantics and causing negative video features to become systematically misaligned with the correct answer at the semantic level, intentionally inducing semantic-level hallucinations.

### 4.3. Spatiotemporal-Semantic Disruptor

To effectively disrupt video features, we introduce Spatiotemporal-Semantic Disruptor, a lightweight neural network consisting of only a few linear and nonlinear layers (see Appendix A for architectural details). During training, the overall loss is defined as:

$$\mathcal{L} = \mathcal{L}_T + \lambda \mathcal{L}_S. \quad (16)$$

where  $\lambda$  is a hyperparameter that controls the relative weighting between the two loss terms in overall optimization.

Under the formulation in Eq. 5, modeling the disruption in a residual form allows the disruptor to modulate spatiotemporal and semantic information while preserving the overall feature structure, thereby stabilizing training and preventing excessive feature distortion. Moreover, its lightweight design introduces minimal computational overhead, enabling efficient end-to-end training with the backbone frozen.

During inference, we employ the disruptor to guide the decoding process via a contrastive decoding strategy:

$$p_{\text{SSCD}}(\mathbf{Y} \mid \mathbf{Z}_v, \mathbf{Z}_v^{\text{Neg}}, \mathbf{X}) = \text{Softmax} \left[ (1 + \alpha) f_{\theta}(\mathbf{Y} \mid \mathbf{Z}_v, \mathbf{X}) - \alpha f_{\theta}(\mathbf{Y} \mid \mathbf{Z}_v^{\text{Neg}}, \mathbf{X}) \right], \quad (17)$$

where larger  $\alpha$  values amplify the difference between the two distributions. To avoid over-penalizing linguistically plausible tokens, we apply an adaptive plausibility constraint following Leng et al. (2024), which filters the candidate

tokens during decoding as follows:

$$\begin{aligned} \mathcal{V}_H(y_{<t}) &= \{y_t \in \mathcal{V} : \\ p_{\theta}(y_t \mid \mathbf{Z}_v, \mathbf{X}, y_{<t}) &\geq \beta \max_w p_{\theta}(w \mid \mathbf{Z}_v, \mathbf{X}, y_{<t})\}, \quad (18) \\ p_{\text{SSCD}}(y_t \mid \mathbf{Z}_v, \mathbf{Z}_v^{\text{Neg}}, \mathbf{X}) &= 0, \text{ if } y_t \notin \mathcal{V}_H(y_{<t}), \end{aligned}$$

where  $\beta \in [0, 1]$  controls the truncation strength. A larger value of  $\beta$  indicates that only tokens with higher probabilities are retained. Under a reasonable plausibility constraint, the final sampling distribution is defined as

$$y_t \sim \text{Softmax} \left[ (1 + \alpha) f_{\theta}(y_t \mid \mathbf{Z}_v, \mathbf{X}, y_{<t}) - \alpha f_{\theta}(y_t \mid \mathbf{Z}_v^{\text{Neg}}, \mathbf{X}, y_{<t}) \right] \text{ s.t. } y_t \in \mathcal{V}_H(y_{<t}). \quad (19)$$

Unlike existing methods, SSCD is theoretically grounded and leverages random walks and conditional mutual information to characterize and disrupt spatiotemporal and semantic consistency in video features. It then calibrates the generation distribution using deliberately disrupted negative video features, thereby effectively mitigating video hallucinations.

## 5. Experiments

In this section, we conduct a comprehensive evaluation of SSCD against representative methods to rigorously assess its effectiveness in mitigating video hallucinations while preserving general video understanding and reasoning capabilities. We further present ablation studies and qualitative analyses to gain deeper insights into the contributions of individual components and the overall behavior of SSCD.

### 5.1. Experimental Setup

**Models and Baselines** We adopt Video-LLaVA (8 frames) (Lin et al., 2024) and LLaVA-NeXT-Video (16 frames) (Zhang et al., 2024b), both with 7B parameters, as our backbone models. In addition to the vanilla VideoLLMs, we compare the proposed method with several representative baselines for video hallucination mitigation, including TCD (Li et al., 2025a), MotionCD (Kong et al., 2025), and Dino-Heal (Zhang et al., 2024a).

**Evaluations** We adopt VideoHalluciner (Wang et al., 2024), EventHallusion (Zhang et al., 2024a), and VideoHallu (Li et al., 2025c) as representative benchmarks to comprehensively evaluate hallucination mitigation performance across diverse video hallucination settings. In addition, ActivityNet-QA (Yu et al., 2019) is used to assess video understanding ability, while MMVU (Zhao et al., 2025b) evaluates video reasoning ability, together providing a thorough and well-rounded evaluation. For EventHallusion, we follow Cai et al. (2025); Wu et al. (2025a) and reproduce only the deterministic subtasks to reduce ambiguity

Table 1. Results on VideoHalluciner and EventHallusion benchmarks. \* and \* indicate metrics for which values closer to 0 and 0.5, respectively, are better; others are higher-is-better. Best and second-best results are highlighted in bold and underlined, respectively. Overall, our method consistently achieves the best or second-best performance across most metrics on both benchmarks, indicating improved robustness against diverse hallucination types.

Method	VideoHalluciner								EventHallusion			
	ORH	TH	SDH	EFH	ENFH	Overall	Pct. Diff*	FP Ratio*	Entire	Mix	Misl.	Overall
Video-LLaVA	35.5	9.7	11.0	3.0	24.0	14.3	0.36	0.92	31.6	<u>57.5</u>	43.1	46.7
+ TCD	<u>36.0</u>	10.2	9.5	4.0	25.5	14.6	0.36	0.92	29.8	56.5	41.2	45.2
+ MotionCD	45.0	<u>15.9</u>	<b>23.5</b>	<b>9.5</b>	<u>26.0</u>	<u>20.5</u>	<u>0.25</u>	<u>0.78</u>	32.5	48.7	33.3	40.3
+ Dino-Heal	<u>36.0</u>	10.2	12.0	4.0	25.0	15.0	0.36	0.92	29.8	<b>59.6</b>	<u>44.1</u>	47.4
+ Ours	<b>46.5</b>	<b>29.5</b>	<u>21.0</u>	<u>8.0</u>	<b>30.0</b>	<b>22.9</b>	<b>0.20</b>	<b>0.75</b>	<b>45.6</b>	51.3	<b>67.6</b>	<b>53.8</b>
LLaVA-NeXT	58.0	21.6	47.0	15.5	46.0	32.3	0.16	0.73	46.5	<b>52.3</b>	44.1	48.7
+ TCD	<u>58.5</u>	<u>23.3</u>	<u>47.0</u>	12.5	<b>47.0</b>	<u>32.3</u>	0.16	0.72	45.6	<u>51.8</u>	47.1	<u>50.9</u>
+ MotionCD	48.5	20.5	34.5	13.5	28.0	24.8	<u>0.06</u>	<u>0.58</u>	44.7	42.5	50.0	45.0
+ Dino-Heal	6.0	22.7	2.5	<u>18.0</u>	25.0	12.4	-0.11	0.38	<b>84.2</b>	4.7	<b>93.1</b>	48.9
+ Ours	<b>60.5</b>	<b>32.4</b>	<b>52.0</b>	<b>18.5</b>	44.0	<b>35.4</b>	<b>-0.04</b>	<b>0.44</b>	<u>50.9</u>	48.2	<u>57.8</u>	<b>51.3</b>

Table 2. Results on VideoHallu benchmark. Higher values indicate better performance across all metrics. Best and second-best results are highlighted in bold and underlined, respectively. Notably, our method attains the best or second-best performance on most metrics and achieves the top overall performance among all compared methods.

Method	Alignment				S-T Consistency			Commonsense		Physics				Overall
	EC	EP	ERAC	SR	CD	SD	TD	K	R	C	CAP	M	ST	
Video-LLaVA	<u>41.1</u>	<b>49.3</b>	51.7	<b>42.9</b>	<b>23.8</b>	<u>35.2</u>	<u>37.1</u>	34.4	33.3	28.6	29.4	41.1	<u>50.0</u>	<u>40.3</u>
+ TCD	<b>42.7</b>	48.8	<u>52.9</u>	40.5	<b>23.8</b>	32.4	36.0	34.4	36.2	<u>38.1</u>	29.4	42.2	<u>50.0</u>	40.3
+ MotionCD	35.1	38.9	42.0	28.6	16.7	31.7	32.6	<b>41.0</b>	29.0	<b>42.9</b>	<u>41.2</u>	34.4	10.0	34.6
+ Dino-Heal	40.0	42.9	42.0	33.3	21.4	25.3	27.7	31.2	24.6	33.3	11.8	33.3	<u>50.0</u>	33.0
+ Ours	36.8	46.8	<b>59.2</b>	<b>42.9</b>	<b>23.8</b>	<b>35.9</b>	<b>38.8</b>	<u>39.3</u>	<b>44.9</b>	<u>38.1</u>	<b>47.1</b>	<b>45.6</b>	<b>70.0</b>	<b>42.4</b>
LLaVA-NeXT	<b>40.0</b>	<b>49.3</b>	50.0	33.3	<b>33.3</b>	<u>33.1</u>	30.3	39.3	<u>34.8</u>	33.3	29.4	<b>34.4</b>	70.0	37.8
+ TCD	35.7	47.3	47.7	<b>35.7</b>	<b>33.3</b>	31.7	<u>30.7</u>	41.0	31.9	<b>42.9</b>	<b>47.1</b>	31.1	<b>80.0</b>	36.9
+ MotionCD	32.4	40.0	50.0	33.3	31.0	31.7	29.2	<b>42.6</b>	29.0	33.3	<u>35.3</u>	27.8	50.0	34.5
+ Dino-Heal	36.8	45.3	<u>54.6</u>	31.0	28.6	<b>33.8</b>	29.2	41.0	<u>34.8</u>	33.3	29.4	<u>33.3</u>	60.0	36.9
+ Ours	<u>37.3</u>	<u>46.3</u>	<b>56.3</b>	<b>35.7</b>	23.8	31.7	<b>31.6</b>	<b>42.6</b>	<b>43.5</b>	<u>38.1</u>	<u>35.3</u>	30.0	<b>80.0</b>	<b>38.3</b>

during evaluation. For evaluation metrics that require an LLM-as-judge, we use the originally specified model and hyperparameters. Detailed descriptions of the evaluation procedure and benchmarks are provided in Appendix B.

**Implementation Details** We randomly sample 3,000 instances from ShareGPT4Video (Chen et al., 2024) to train the disruptor. Following Jabri et al. (2020), we set the hyperparameter  $\tau$  in Eq. 7 to 0.07, and the coefficient  $\lambda$  in Eq. 16 to 5. The parameter  $\alpha$  in Eq. 17 is set to 0.8 for Video-LLaVA and 0.4 for LLaVA-NeXT-Video, while  $\beta$  in Eq. 18 is fixed at 0.1. During inference, we set the maximum token length to 512 and adopt greedy decoding as the default inference strategy to ensure stability and reproducibility. Additional details are provided in Appendix C.

## 5.2. Main Results

**Video Hallucination Mitigation** As shown in Tables 1 and 2, our method achieves the best overall performance across all three video hallucination evaluation benchmarks.

On VideoHalluciner, our approach effectively mitigates hallucinations while also substantially reducing model bias. On EventHallusion, Dino-Heal shows strong performance on the Entire and Misl. metrics when combined with LLaVA-NeXT-Video. However, its performance on the Mix metric is noticeably weaker, which limits its overall effectiveness compared to our method. In addition, when applied to LLaVA-NeXT-Video, Dino-Heal performs poorly on both the ORH and SDH metrics, indicating limited generalization ability of this heuristic-based design. Furthermore, our method is the only one that achieves an overall performance improvement over the vanilla model on VideoHallu. Taken together, these results indicate that SSCD is more effective at mitigating video hallucinations than the baseline methods.

**Video Understanding and Reasoning** We further evaluate the impact of SSCD on the model’s general video understanding and reasoning abilities, with results summarized in Table 3. Notably, for Video-LLaVA, SSCD consistently improves performance across both datasets and achieves the best overall results among all competing methods. For

Table 3. Results on ActivityNet-QA and MMVU benchmarks. Higher values indicate better performance across all metrics.

Method	ActivityNet-QA		MMVU	
	Accuracy	Score	Direct	CoT
Video-LLaVA	40.9	2.95	29.0	28.2
+ TCD	40.3	2.94	28.7	28.6
+ MotionCD	39.0	2.82	27.6	27.2
+ Dino-Heal	40.7	2.92	28.7	29.2
+ Ours	41.5	2.98	32.0	28.5
LLaVA-NeXT	53.3	3.43	31.3	30.5
+ TCD	49.1	3.10	25.6	29.8
+ MotionCD	45.0	2.92	26.3	25.1
+ Dino-Heal	53.0	3.38	30.9	30.7
+ Ours	53.3	3.31	31.1	30.1

Table 4. Ablation results of spatiotemporal (S1) and semantic (S2) consistency disruption on EventHallusion benchmark.

Backbone	S1	S2	Entire	Mix	Misl.	OA
Video-LLaVA	×	×	31.6	57.5	43.1	46.7
	✓	×	39.5	51.3	66.7	51.8
	✓	✓	45.6	51.3	67.6	53.8
LLaVA-NeXT	×	×	46.5	52.3	44.1	48.7
	✓	×	44.7	57.0	46.1	50.9
	✓	✓	50.9	48.2	57.8	51.3

LLaVA-NeXT-Video, SSCD largely maintains performance on both datasets, whereas alternative approaches, with the exception of Dino-Heal, result in noticeable performance degradation. Overall, Dino-Heal and our method demonstrate comparable performance on the two datasets. Importantly, SSCD shows a clear advantage in suppressing video hallucinations, effectively alleviating hallucination issues while largely preserving the model’s general video understanding and reasoning capabilities.

### 5.3. Ablation Study

#### Effects of Spatiotemporal and Semantic Disruptions

Table 4 reports the ablation results of spatiotemporal consistency disruption and semantic consistency disruption. When both objectives are removed, corresponding to the vanilla model, the overall performance drops to the lowest level. Applying only spatiotemporal consistency disruption already leads to clear improvements on the Entire and Misl. metrics, which translates into an overall performance gain. Further introducing semantic consistency disruption on top of spatiotemporal disruption brings additional overall improvements. These results demonstrate that both spatiotemporal and semantic consistency disruption contribute positively to the final performance.

**Ablations on Hyperparameters** We conduct ablation studies on the hyperparameters of SSCD using Video-

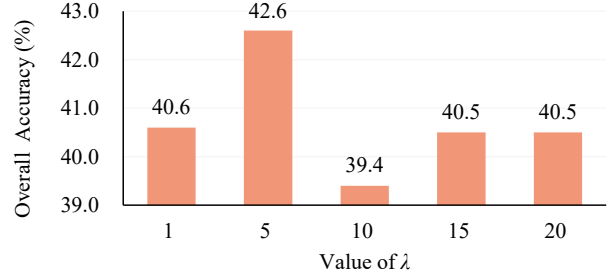


Figure 2. Ablation analysis of  $\lambda$  in training on the direct multiple-choice subset of MMVU with Video-LLaVA as the backbone.

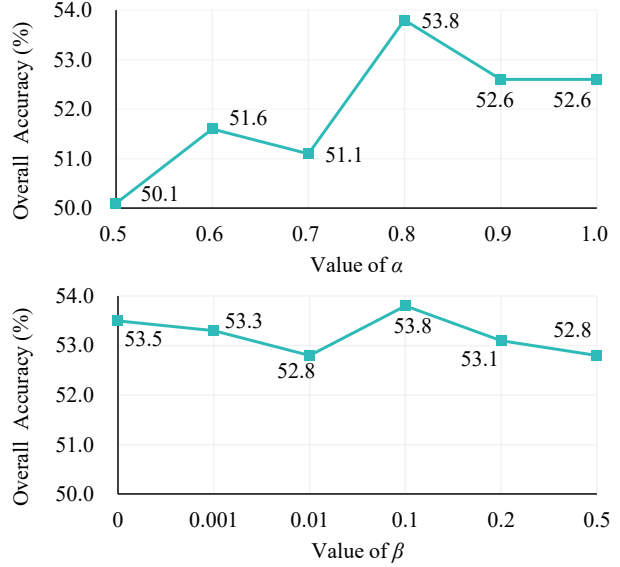


Figure 3. Ablation analysis of  $\alpha$  and  $\beta$  in contrastive decoding on EventHallusion using Video-LLaVA as the backbone.

LLaVA. Since the parameters  $\tau$  in Eq. 7 and  $\lambda$  in Eq. 16 only influence the gradients of the loss terms during training, we fix  $\tau$  and vary  $\lambda$  to examine its impact on the direct multiple-choice subset of MMVU. As shown in Figure 2, performance improves as  $\lambda$  increases from 1 to 5, while further increasing  $\lambda$  leads to performance degradation and eventually results in a plateau.

We also investigate the effects of  $\alpha$  in Eq. 17 and  $\beta$  in Eq. 18 on EventHallusion, as illustrated in Figure 3. Increasing the contrastive strength  $\alpha$  from 0.5 to 0.8 consistently improves performance, whereas larger values cause performance degradation, indicating that excessive correction is harmful. In contrast, varying  $\beta$  produces only marginal changes in performance, suggesting that the method is relatively robust to the choice of this parameter.

### 5.4. Case Study

To qualitatively analyze the behavior of SSCD, we present two representative examples in Figures 4 and 5, where the

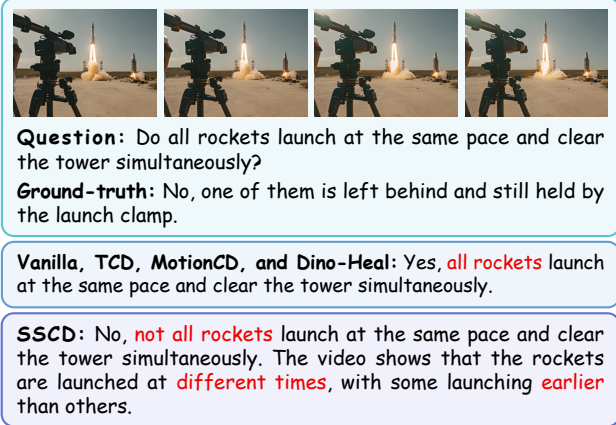


Figure 4. An example from the VideoHallu dataset with LLaVA-NeXT-Video as the backbone, where SSCD demonstrates superior temporal information modeling compared to the baseline.

predictions of SSCD are compared against those of several baseline methods.

In the first example shown in Figure 4, the video shows two rockets that do not launch and clear the tower simultaneously. When asked whether all rockets launch at the same time, all baseline methods incorrectly predict a synchronized launch, contradicting the ground truth. In contrast, SSCD correctly identifies that the launches are not simultaneous. This result suggests that the baseline errors arise from insufficient temporal reasoning, whereas SSCD exhibits greater robustness in modeling temporal order.

The second example in Figure 5 presents a dental procedure consisting of multiple operational steps. Baseline methods yield highly inconsistent predictions regarding the type of procedure. Some methods focus predominantly on the observed drilling operation and mistakenly classify the procedure as tooth extraction, while MotionCD hallucinates nonexistent procedural steps, leading to an incorrect interpretation. By contrast, SSCD grounds its prediction in a sequence of key operations visible in the video, such as pulp removal and filling, and aligns this temporal evidence with the standard workflow of root canal treatment. This results in a factually consistent conclusion. This example indicates that baseline failures often stem from over-reliance on isolated visual cues or hallucinated procedural completion, whereas SSCD effectively suppresses video hallucinations by enforcing temporal consistency.

Overall, these two examples demonstrate that the evaluated baseline VideoLLMs are prone to producing predictions that are inconsistent with the video content when reasoning about temporal order or multi-step processes. In contrast, SSCD alleviates such inconsistencies, providing qualitative evidence that supports its quantitative performance. Additional representative cases are provided in Appendix D.

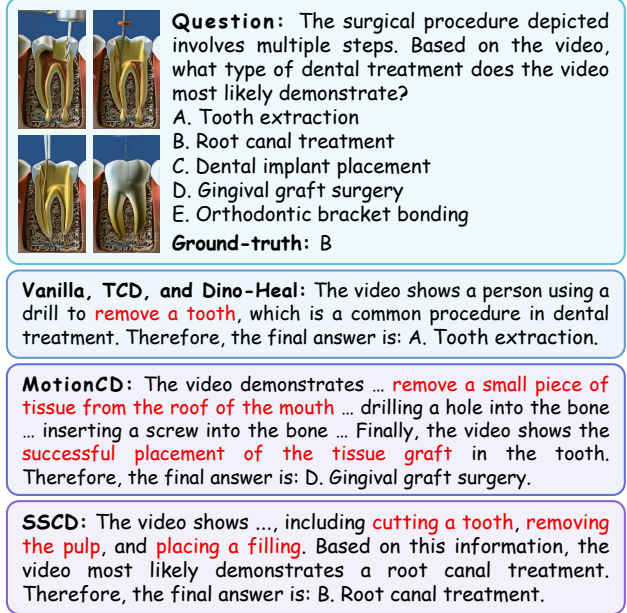


Figure 5. An example from the MMVU dataset using VideoLLaVA as the backbone. Compared with the baseline, SSCD accurately captures key information across multiple operational steps and correctly interprets and associates it based on domain-specific knowledge.

## 6. Conclusion

This work investigates hallucinations in VideoLLMs and introduces SSCD, a decoding strategy that mitigates hallucinations without modifying or retraining the backbone model. SSCD deliberately perturbs spatiotemporal consistency and semantic alignment to construct hallucination-prone negative video features, which are integrated into a contrastive decoding framework to suppress hallucinated outputs.

Extensive experiments on multiple benchmarks demonstrate that SSCD consistently outperforms existing decoding-based methods in reducing hallucination rates, while largely preserving general video understanding and reasoning capabilities. Despite its effectiveness, SSCD has several limitations. Its performance depends on the contrastive signals introduced during decoding and is inherently constrained by the quality of the underlying video representations. When video encodings lack sufficient discriminative information, the potential for effective hallucination mitigation is reduced. Moreover, SSCD is sensitive to hyperparameters such as the contrastive strength, which may require careful calibration across different tasks and model architectures.

Overall, SSCD offers a lightweight and modular solution for improving the reliability of VideoLLMs without requiring any modifications to the backbone model. This work highlights the benefits of explicitly modeling hallucination-related factors during decoding.



## Impact Statement

This paper presents work whose goal is to advance the field of Machine Learning. There are many potential societal consequences of our work, none which we feel must be specifically highlighted here.

## References

- Bae, K., Kim, J., Lee, S., Lee, S., Lee, G., and Choi, J. Mash-  
vlm: Mitigating action-scene hallucination in video-llms  
through disentangled spatial-temporal representations. In  
*Proceedings of the Computer Vision and Pattern Recog-  
nition Conference*, pp. 13744–13753, 2025.
- Bagad, P., Tapaswi, M., and Snoek, C. G. Test of time:  
Instilling video-language models with a sense of time. In  
*Proceedings of the IEEE/CVF Conference on Computer  
Vision and Pattern Recognition*, pp. 2503–2516, 2023.
- Cai, J., Zhou, W., Zhang, Z., Hong, J., Zhan, N., and Li, H.  
Mitigating hallucination in videollms via temporal-aware  
activation engineering. *arXiv preprint arXiv:2505.12826*,  
2025.
- Chen, L., Wei, X., Li, J., Dong, X., Zhang, P., Zang,  
Y., Chen, Z., Duan, H., Tang, Z., Yuan, L., et al.  
Sharegpt4video: Improving video understanding and gen-  
eration with better captions. *Advances in Neural Infor-  
mation Processing Systems*, 37:19472–19495, 2024.
- Chen, W., Yan, X., Wen, B., Yang, F., Gao, T., Zhang, D.,  
and Chen, L. Decoupling contrastive decoding: Robust  
hallucination mitigation in multimodal large language  
models. *arXiv preprint arXiv:2504.08809*, 2025.
- Cui, Z., Yuan, J., Wang, H., Li, Y., Du, C., and Ding, Z.  
Draw with thought: Unleashing multimodal reasoning  
for scientific diagram generation. In *Proceedings of the  
33rd ACM International Conference on Multimedia*, pp.  
5050–5059, 2025.
- Ding, X., Zhang, K., Han, J., Hong, L., Xu, H., and Li, X.  
Pami-vdpo: Mitigating video hallucinations by prompt-  
aware multi-instance video preference learning. *arXiv  
preprint arXiv:2504.05810*, 2025.
- Fang, H., Zhou, C., Kong, J., Gao, K., Chen, B., Liang, T.,  
Ma, G., and Xia, S.-T. Grounding language with vision: A  
conditional mutual information calibrated decoding strat-  
egy for reducing hallucinations in lvlms. *arXiv preprint  
arXiv:2505.19678*, 2025.
- Fu, J., Fei, H., Shen, X., Hooi, B., Qiu, X., Ng, S.-K.,  
et al. Chip: Cross-modal hierarchical direct preference  
optimization for multimodal llms. In *The Thirteenth  
International Conference on Learning Representations*,  
2025.
- Gao, H., Qu, J., Tang, J., Bi, B., Liu, Y., Chen, H., Liang, L.,  
Su, L., and Huang, Q. Exploring hallucination of large  
multimodal models in video understanding: Benchmark,  
analysis and mitigation. *arXiv preprint arXiv:2503.19622*,  
2025a.
- Gao, P., Han, J., Zhang, R., Lin, Z., Geng, S., Zhou, A.,  
Zhang, W., Lu, P., He, C., Yue, X., et al. Llama-adapter  
v2: Parameter-efficient visual instruction model. *arXiv  
preprint arXiv:2304.15010*, 2023.
- Gao, Y., Bao, H., Zhang, T., Li, B., Wang, Z., and Chen, W.  
Mentalmac: Enhancing large language models for detect-  
ing mental manipulation via multi-task anti-curriculum  
distillation. *arXiv preprint arXiv:2505.15255*, 2025b.
- Gunjal, A., Yin, J., and Bas, E. Detecting and prevent-  
ing hallucinations in large vision language models. In  
*Proceedings of the AAAI Conference on Artificial Intelli-  
gence*, volume 38, pp. 18135–18143, 2024.
- Huang, H., Chen, H., Wu, S., Luo, M., Fu, J., Du, X.,  
Zhang, H., and Fei, H. Vistadpo: Video hierarchical  
spatial-temporal direct preference optimization for large  
video models. *arXiv preprint arXiv:2504.13122*, 2025.
- Jabri, A., Owens, A., and Efros, A. Space-time correspon-  
dence as a contrastive random walk. *Advances in neural  
information processing systems*, 33:19545–19560, 2020.
- Jiang, Z., Chen, J., Zhu, B., Luo, T., Shen, Y., and Yang, X.  
Devils in middle layers of large vision-language models:  
Interpreting, detecting and mitigating object hallucina-  
tions via attention lens. In *Proceedings of the Computer  
Vision and Pattern Recognition Conference*, pp. 25004–  
25014, 2025.
- Kong, M., Zeng, X., Chen, L., Li, Y., Yan, B., and Zhu, Q.  
Mhbench: Demystifying motion hallucination in vide-  
ollms. In *Proceedings of the AAAI Conference on Arti-  
ficial Intelligence*, volume 39, pp. 4401–4409, 2025.
- Lee, S., Park, S. H., Jo, Y., and Seo, M. Volcano: Mitigating  
multimodal hallucination through self-feedback guided  
revision. In *2024 Conference of the North American  
Chapter of the Association for Computational Linguistics:  
Human Language Technologies, NAACL 2024*, pp. 391–  
404. Association for Computational Linguistics (ACL),  
2024.
- Leng, S., Zhang, H., Chen, G., Li, X., Lu, S., Miao, C., and  
Bing, L. Mitigating object hallucinations in large vision-  
language models through visual contrastive decoding. In  
*Proceedings of the IEEE/CVF Conference on Computer  
Vision and Pattern Recognition*, pp. 13872–13882, 2024.

- Li, C., Im, E. W., and Fazli, P. Vidhalluc: Evaluating temporal hallucinations in multimodal large language models for video understanding. In *Proceedings of the Computer Vision and Pattern Recognition Conference*, pp. 13723–13733, 2025a.
- Li, J., Li, D., Xiong, C., and Hoi, S. Blip: Bootstrapping language-image pre-training for unified vision-language understanding and generation. In *International conference on machine learning*, pp. 12888–12900. PMLR, 2022.
- Li, Z., Shi, H., Gao, Y., Liu, D., Wang, Z., Chen, Y., Liu, T., Zhao, L., Wang, H., and Metaxas, D. N. The hidden life of tokens: Reducing hallucination of large vision-language models via visual information steering. In *Forty-second International Conference on Machine Learning*, 2025b.
- Li, Z., Wu, X., Shi, G., Qin, Y., Du, H., Liu, F., Zhou, T., Manocha, D., and Boyd-Graber, J. L. Videohallu: Evaluating and mitigating multi-modal hallucinations on synthetic video understanding, 2025c.
- Lin, B., Ye, Y., Zhu, B., Cui, J., Ning, M., Jin, P., and Yuan, L. Video-llava: Learning united visual representation by alignment before projection. In *Proceedings of the 2024 Conference on Empirical Methods in Natural Language Processing*, pp. 5971–5984, 2024.
- Liu, F., Lin, K., Li, L., Wang, J., Yacoob, Y., and Wang, L. Mitigating hallucination in large multi-modal models via robust instruction tuning. In *The Twelfth International Conference on Learning Representations*, 2024a.
- Liu, Y., Li, S., Liu, Y., Wang, Y., Ren, S., Li, L., Chen, S., Sun, X., and Hou, L. Tempcompass: Do video llms really understand videos? In *Findings of the Association for Computational Linguistics ACL 2024*, pp. 8731–8772, 2024b.
- Loshchilov, I. and Hutter, F. Decoupled weight decay regularization. *arXiv preprint arXiv:1711.05101*, 2017.
- Ma, F., Jin, X., Wang, H., Xian, Y., Feng, J., and Yang, Y. Vista-llama: Reducing hallucination in video language models via equal distance to visual tokens. In *Proceedings of the IEEE/CVF Conference on Computer Vision and Pattern Recognition*, pp. 13151–13160, 2024.
- Maaz, M., Rasheed, H., Khan, S., and Khan, F. Videochatgpt: Towards detailed video understanding via large vision and language models. In *Proceedings of the 62nd Annual Meeting of the Association for Computational Linguistics (Volume 1: Long Papers)*, pp. 12585–12602, 2024.
- Poppi, T., Uzkont, B., Garg, A., Porto, L., Kessler, G., Yang, Y., Cornia, M., Baraldi, L., Cucchiara, R., and Schiffers, F. Countervid: Counterfactual video generation for mitigating action and temporal hallucinations in video-language models. *arXiv preprint arXiv:2601.04778*, 2026.
- Radford, A., Kim, J. W., Hallacy, C., Ramesh, A., Goh, G., Agarwal, S., Sastry, G., Askell, A., Mishkin, P., Clark, J., et al. Learning transferable visual models from natural language supervision. In *International conference on machine learning*, pp. 8748–8763. PmLR, 2021.
- Rafailov, R., Sharma, A., Mitchell, E., Manning, C. D., Ermon, S., and Finn, C. Direct preference optimization: Your language model is secretly a reward model. *Advances in neural information processing systems*, 36: 53728–53741, 2023.
- Shah, J., Bikshandi, G., Zhang, Y., Thakkar, V., Ramani, P., and Dao, T. Flashattention-3: Fast and accurate attention with asynchrony and low-precision. *Advances in Neural Information Processing Systems*, 37:68658–68685, 2024.
- Sun, Y., Zhang, M., Li, F., Hong, G., and Yang, M. Smart-sight: Mitigating hallucination in video-llms without compromising video understanding via temporal attention collapse. *arXiv preprint arXiv:2512.18671*, 2025.
- Tang, F., Liu, C., Xu, Z., Hu, M., Huang, Z., Xue, H., Chen, Z., Peng, Z., Yang, Z., Zhou, S., et al. Seeing far and clearly: Mitigating hallucinations in mllms with attention causal decoding. In *Proceedings of the Computer Vision and Pattern Recognition Conference*, pp. 26147–26159, 2025.
- Vaswani, A., Shazeer, N., Parmar, N., Uszkoreit, J., Jones, L., Gomez, A. N., Kaiser, L. u., and Polosukhin, I. Attention is all you need. In *Advances in Neural Information Processing Systems*, volume 30, 2017.
- Wang, H., Wang, S., Zhong, Y., Yang, Z., Wang, J., Cui, Z., Yuan, J., Han, Y., Liu, M., and Ma, Y. Affordancerl: Reinforcement learning for generalizable affordance reasoning in multimodal large language model. *arXiv preprint arXiv:2508.06206*, 2025.
- Wang, Y., Wang, Y., Zhao, D., Xie, C., and Zheng, Z. Videohalluc: Evaluating intrinsic and extrinsic hallucinations in large video-language models. *arXiv preprint arXiv:2406.16338*, 2024.
- Wu, C.-H., Chang, K.-P., Sheng, Y.-Y., Chung, H.-K., Wang, K.-C., and Wang, Y.-C. F. Season: Mitigating temporal hallucination in video large language models via self-diagnostic contrastive decoding. *arXiv preprint arXiv:2512.04643*, 2025a.

- Wu, Z., Chen, Z., Luo, R., Zhang, C., Gao, Y., He, Z., Wang, X., Lin, H., and Qiu, M. Valley2: Exploring multimodal models with scalable vision-language design. *arXiv preprint arXiv:2501.05901*, 2025b.
- Xu, L., Zhao, Y., Zhou, D., Lin, Z., Ng, S. K., and Feng, J. Pllava: Parameter-free llava extension from images to videos for video dense captioning. *arXiv preprint arXiv:2404.16994*, 2024.
- Yu, Q., Li, J., Wei, L., Pang, L., Ye, W., Qin, B., Tang, S., Tian, Q., and Zhuang, Y. Hallucidoctor: Mitigating hallucinatory toxicity in visual instruction data. In *Proceedings of the IEEE/CVF Conference on Computer Vision and Pattern Recognition*, pp. 12944–12953, 2024.
- Yu, Z., Xu, D., Yu, J., Yu, T., Zhao, Z., Zhuang, Y., and Tao, D. Activitynet-qa: A dataset for understanding complex web videos via question answering. In *Proceedings of the AAAI Conference on Artificial Intelligence*, volume 33, pp. 9127–9134, 2019.
- Yuan, F., Qin, C., Xu, X., and Li, P. Helpd: Mitigating hallucination of lvlms by hierarchical feedback learning with vision-enhanced penalty decoding. In *Proceedings of the 2024 Conference on Empirical Methods in Natural Language Processing*, pp. 1768–1785, 2024.
- Yuan, J., Cui, Z., Wang, H., Gao, Y., Zhou, Y., and Naseem, U. Kardia-r1: Unleashing llms to reason toward understanding and empathy for emotional support via rubric-as-judge reinforcement learning. *arXiv preprint arXiv:2512.01282*, 2025a.
- Yuan, J., Du, D., Zhang, H., Di, Z., and Naseem, U. Reversal of thought: Enhancing large language models with preference-guided reverse reasoning warm-up. In *Proceedings of the 63rd Annual Meeting of the Association for Computational Linguistics (Volume 1: Long Papers)*, pp. 19442–19459, 2025b.
- Yue, Z., Zhang, L., and Jin, Q. Less is more: Mitigating multimodal hallucination from an eos decision perspective. In *Proceedings of the 62nd Annual Meeting of the Association for Computational Linguistics (Volume 1: Long Papers)*, pp. 11766–11781, 2024.
- Zhang, H., Li, X., and Bing, L. Video-llama: An instruction-tuned audio-visual language model for video understanding. In *Proceedings of the 2023 Conference on Empirical Methods in Natural Language Processing: System Demonstrations*, pp. 543–553, 2023.
- Zhang, J., Jiao, Y., Chen, S., Zhao, N., Tan, Z., Li, H., and Chen, J. Eventhallusion: Diagnosing event hallucinations in video llms. *arXiv preprint arXiv:2409.16597*, 2024a.
- Zhang, S., Fang, Q., Yang, Z., and Feng, Y. Llava-mini: Efficient image and video large multimodal models with one vision token. In *The Thirteenth International Conference on Learning Representations*, 2025.
- Zhang, Y., Li, B., Liu, h., Lee, Y. j., Gui, L., Fu, D., Feng, J., Liu, Z., and Li, C. Llava-next: A strong zero-shot video understanding model, April 2024b. URL <https://llava-vl.github.io/blog/2024-04-30-llava-next-video/>.
- Zhao, S., Wang, Y., Yang, Z., and Cai, D. Region mutual information loss for semantic segmentation. *Advances in Neural Information Processing Systems*, 32, 2019.
- Zhao, S., Yuan, J., Wu, J., Wang, Z., Yang, G., and Naseem, U. Can pruning improve reasoning? revisiting long-cot compression with capability in mind for better reasoning. *arXiv preprint arXiv:2505.14582*, 2025a.
- Zhao, Y., Zhang, H., Xie, L., Hu, T., Gan, G., Long, Y., Hu, Z., Chen, W., Li, C., Xu, Z., Wang, C., Shangguan, Z., Liang, Z., Liu, Y., Zhao, C., and Cohan, A. Mmvu: Measuring expert-level multi-discipline video understanding. In *Proceedings of the IEEE/CVF Conference on Computer Vision and Pattern Recognition (CVPR)*, pp. 8475–8489, June 2025b.
- Zheng, H., Xu, T., Sun, H., Pu, S., Chen, R., and Sun, L. Thinking before looking: Improving multimodal llm reasoning via mitigating visual hallucination. *arXiv preprint arXiv:2411.12591*, 2024.
- Zhu, B., Lin, B., Ning, M., Yan, Y., Cui, J., HongFa, W., Pang, Y., Jiang, W., Zhang, J., Li, Z., et al. Languagebind: Extending video-language pretraining to n-modality by language-based semantic alignment. In *The Twelfth International Conference on Learning Representations*, 2024.

## A. Architecture of Spatiotemporal-Semantic Disruptor

The details of the disruptor we designed are shown in Figure 6. Notably, this learnable component constitutes only a small portion of the VideoLLM’s total parameters, resulting in minimal computational overhead.

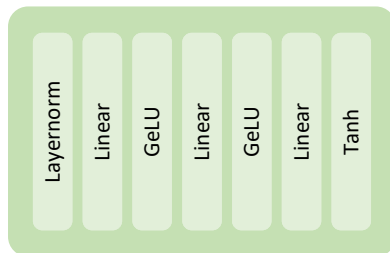


Figure 6. Overview of the architecture of SSD.

## B. Evaluation and Benchmarks

**VideoHalluciner Evaluation** VideoHalluciner comprises both basic questions and hallucination-oriented questions, enabling not only the assessment of hallucination severity but also the analysis of model biases. Specifically, VideoHalluciner evaluates multiple types of hallucinations, including Object-Relation Hallucination (ORH), Temporal Hallucination (TH), Semantic Detail Hallucination (SDH), Extrinsic Factual Hallucination (EFH), and Extrinsic Non-factual Hallucination (ENFH). For each video, a prediction is considered correct only if the model answers both the corresponding basic question and the hallucination question correctly, based on which the overall accuracy is computed. In addition, VideoHalluciner reveals model biases by measuring the Yes Percentage Difference (Pct. Diff) and the False Positive Ratio (FP Ratio). Notably, all evaluation metrics are computed without adopting an LLM-as-Judge paradigm.

**EventHallusion Evaluation** EventHallusion is a benchmark for diagnosing event-level hallucinations in videoLLMs, focusing on failures in understanding temporally unfolding events and action sequences. It comprises 400 videos and 711 human-annotated questions across diverse domains including daily life, sports, transportation, food, animals, and natural scenes. The benchmark is structured into three settings: Entire, Mix, and Misleading (Misl.). During evaluation, the selected deterministic subtasks compute accuracy solely based on binary labels, without relying on an LLM-as-Judge, thereby ensuring objective and consistent evaluation.

**VideoHallu Evaluation** VideoHallu is a benchmark for evaluating and mitigating multi-modal hallucinations in synthetic video understanding. It organizes questions into four categories: Alignment, Spatial-Temporal Consistency, Common Sense Reasoning, and Physics, covering hallucination patterns driven by language priors rather than visual evidence. In addition, Alignment is further divided into Entity Counting (EC), Entity Properties (EP), Entity Recognition & Classification (ERAC), and Spatial Relationships (SR). Spatial-Temporal Consistency is further categorized into Camera Dynamics (CD), Spatial Dynamics (SD), and Temporal Dynamics (TD). Common Sense Reasoning is further divided into Knowledge (K) and Reasoning (R). Physics is further categorized into Conservation (C), Constraints & Properties (CAP), Motion (M), and State Transition (ST). Evaluation is conducted using GPT-4 as an LLM-as-a-Judge to assess the consistency between model outputs and human-annotated ground truth.

**ActivityNet-QA Evaluation** ActivityNet-QA is a classic benchmark dataset for video question answering research, focusing on evaluating models’ abilities in temporal understanding and semantic reasoning over videos. Following Maaz et al. (2024), we conduct zero-shot question answering evaluation on this benchmark using GPT-3.5-Turbo with the same prompt template, and report Accuracy and Score.

**MMVU Evaluation** MMVU is a multi-disciplinary benchmark for expert-level video understanding, evaluating multimodal large models on knowledge-intensive videos from specialized domains. It contains both multiple-choice and open-ended questions, and supports two evaluation settings: Direct answer generation and Chain-of-Thought (CoT) reasoning. For multiple-choice questions under the Direct setting, evaluation does not rely on an LLM-as-Judge, while all other settings are evaluated using GPT-4o.



## C. Implementation Details

Experiments are conducted on two NVIDIA H800 GPUs using the AdamW optimizer (Loshchilov & Hutter, 2017). A warmup ratio of 0.05 is used, followed by a constant learning rate. The disruptor is trained for 3 epochs with a batch size of 2, and 2 gradient accumulation steps. For Video-LLaVA, the learning rate is set to 1e-6, while for LLaVA-NeXT-Video, it is set to 5e-6. For all baselines, we adopt the parameter settings reported in their original papers to ensure a fair comparison.

## D. Representative Examples and Analysis

To provide an intuitive illustration of the proposed method, we select several representative examples from different datasets and present them in Figures 7, 8, 9, and 10. These qualitative results further demonstrate the effectiveness of our method.



Figure 7. An example from the EventHallusion (left) and VideoHalluciner (right) datasets using LLaVA-NeXT-Video as the backbone.

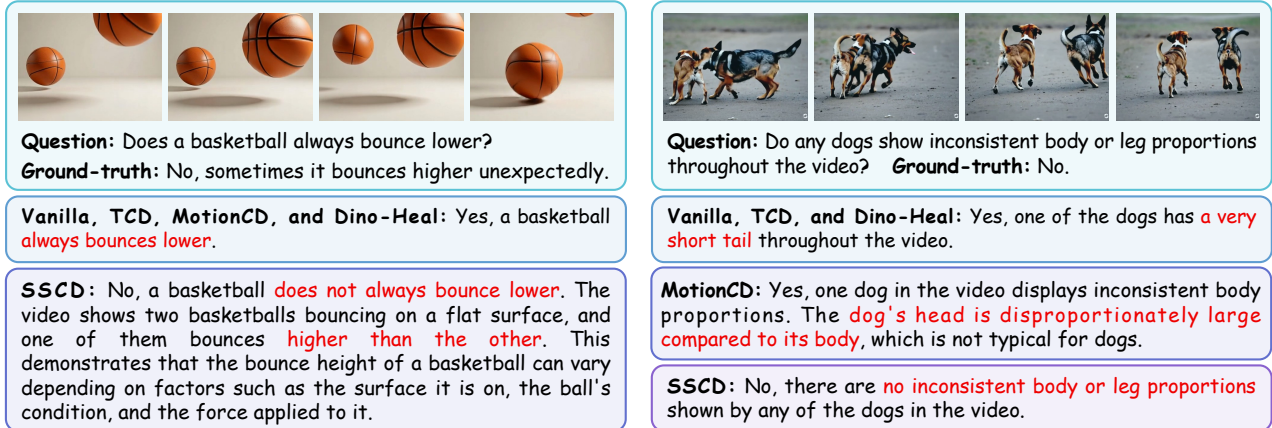


Figure 8. An example from the VideoHallu dataset using LLaVA-NeXT-Video as the backbone.

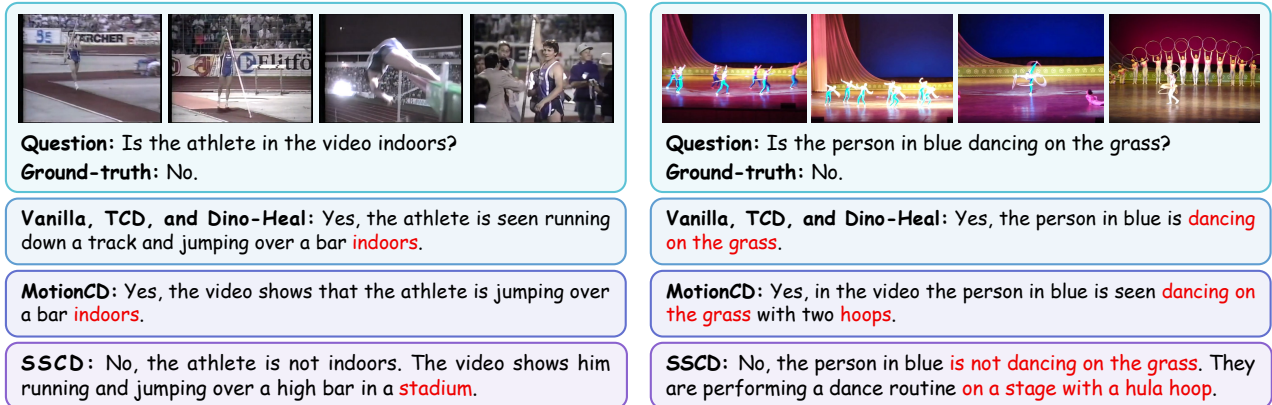
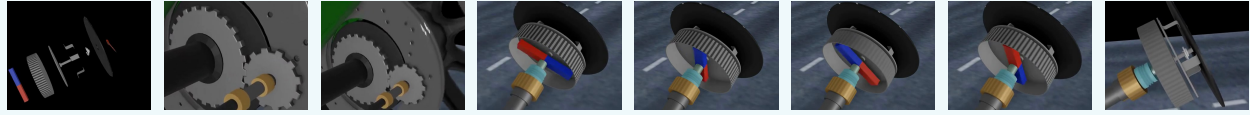


Figure 9. An example from the ActivityNet-QA dataset using Video-LLaVA as the backbone.



**Question:** If a vehicle's wheel diameter is increased without altering the speedometer configuration, how does this modification affect the speedometer reading and why?

- A. The speedometer will read a higher speed than the actual speed because the larger wheels cause the cable to rotate faster.
- B. The speedometer will display the same speed as before, but the actual vehicle speed will be higher for the same reading due to the increased wheel circumference.
- C. The speedometer will automatically adjust and display the correct speed despite the wheel size change.
- D. The speedometer will malfunction because the larger wheels disrupt the magnetic interaction within the speedometer.
- E. The speedometer will read zero because the increased wheel size disengages the speedometer cable.

**Ground-truth:** No.

**Vanilla:** The modification of increasing the wheel diameter without altering the speedometer configuration affects **the speedometer reading by causing the cable to rotate faster**. This is because the larger wheels have a larger circumference, which means that the cable rotates more times before reaching the speedometer. As a result, the speedometer will read a higher speed than the actual speed. Therefore, the final answer is: A. The speedometer will read a higher speed than the actual speed because the larger wheels cause the cable to rotate faster.

**TCD:** The modification of increasing the wheel diameter without altering the speedometer configuration affects the speedometer reading by **causing the cable to rotate faster**. This is because the larger wheels have a larger circumference, which means that the cable rotates more times before reaching the speedometer. Therefore, the speedometer will read a higher speed than the actual speed. Therefore, the final answer is: A.

**MotionCD:** A. The speedometer will read a higher speed than the actual speed because **the larger wheels cause the cable to rotate faster**. The speedometer is designed to measure the rotation of the speedometer cable, which is connected to the wheel. When a vehicle's wheel diameter is increased without altering the speedometer configuration, the speedometer cable's length remains the same. Consequently, the larger wheel causes the cable to rotate faster, which results in the speedometer reading a higher speed than the actual speed. Therefore, the final answer is: A.

**Dino-Heal:** The modification of increasing the wheel diameter without altering the speedometer configuration affects the speedometer reading by causing the cable to rotate faster. This is because the larger wheels have a larger circumference, which means that **the cable rotates more times before reaching the speedometer**. As a result, the speedometer will read a higher speed than the actual speed. Therefore, the final answer is: A. The speedometer will read a higher speed than the actual speed because the larger wheels cause the cable to rotate faster.

**SSCD:** Let's analyze the given information and determine the correct answer. A. The speedometer will read a higher speed than the actual speed because the larger wheels cause the cable to rotate faster. This statement is not correct. The speedometer is designed to measure the speed of the vehicle based on the rotation of the cable. The speedometer does not rely on the cable's rotation speed; it relies on the vehicle's wheel rotation speed. B. The speedometer will display the same speed as before, but the actual vehicle speed will be higher for the same reading due to the increased wheel circumference. This statement is correct. **If a vehicle's wheel diameter is increased without altering the speedometer configuration, the speedometer will display the same speed as before. However, the actual vehicle speed will be higher for the same reading due to the increased wheel circumference.** C. The speedometer will automatically adjust and display the correct speed despite the wheel size change. This statement is not correct. The speedometer is not designed to automatically adjust for changes in wheel size. It relies on the cable's rotation speed to determine the vehicle's speed. D. The speedometer will malfunction because the larger wheels disrupt the magnetic interaction within the speedometer. This statement is not correct. The speedometer does not rely on magnetic interaction; it relies on the cable's rotation speed to determine the vehicle's speed. E. The speedometer will read zero because the increased wheel size disengages the speedometer cable. This statement is not correct. The speedometer does not rely on the cable's rotation speed; it relies on the vehicle's wheel rotation speed. Therefore, the final answer is: B. The speedometer will display the same speed as before, but the actual vehicle speed will be higher for the same reading due to the increased wheel circumference.

Figure 10. An example from the MMVU dataset using Video-LLaVA as the backbone.